# Comparison of tissue oximeters on a liquid phantom with adjustable optical properties

Kleiser, S ; Nasseri, N ; Andresen, B ; Greisen, G ; Wolf, M

DOI: https://doi.org/10.1364/BOE.7.002973

Research Article | Vol. 7, No. 8 | 1 Aug 2016 | BIOMEDICAL OPTICS EXPRESS 2973
Biomedical Optics EXPRESS

# Comparison of tissue oximeters on a liquid phantom with adjustable optical properties

S. KLEISER,[1,3,4] N. NASSERI,[1,3,5] B. ANDRESEN,[2] G. GREISEN,[2] AND M. WOLF[1]

[1]*Biomedical Optics Research Laboratory, Department of Neonatology, University Hospital Zurich, Zurich, Switzerland*
[2]*Department of Neonatology, Copenhagen University Hospital, Rigshospitalet, Copenhagen, Denmark*
[3]*equal contribution*
[4]*stefan.kleiser@usz.ch*
[5]*nassim.nasseri@usz.ch*

**Abstract:** The SafeBoosC trial showed that cerebral oximetry combined with a treatment guideline can reduce the the burden of hypoxia in neonates by 50% [Brit. Med. J. **350**, g7635 (2015)]. However, guidelines based on oximetry by one oximeter are not directly usable by other oximeters. We made a blood-lipid phantom simulating the neonatal head to determine the relation between oxygenation values obtained by different oximeters. We calculated coefficients for easy conversion from one oximeter to the other. We additionally determined the corresponding SafeBoosC intervention thresholds at which we measured an uncertainty of up to 9.2% when varying hemoglobin content from $25\mu M$ to $70\mu M$. In conclusion, this paper makes the comparison of absolute values obtained by different oximeters possible.



**OCIS codes:** (120.3890) Medical optics instrumentation; (170.6510) Spectroscopy, tissue diagnostics.

## References and links

1. J. J. Volpe, "Brain injury in premature infants: a complex amalgam of destructive and developmental disturbances," Lancet Neurol. **8**, 110–124 (2009).
2. S. Hyttel-Sorensen, A. Pellicer, T. Alderliesten, T. Austin, F. van Bel, M. Benders, O. Claris, E. Dempsey, A. R. Franz, M. Fumagalli, C. Gluud, B. Grevstad, C. Hagmann, P. Lemmers, W. van Oeveren, G. Pichler, A. M. Plomgaard, J. Riera, L. Sanchez, P. Winkel, M. Wolf, and G. Greisen, "Cerebral near infrared spectroscopy oximetry in extremely preterm infants: Phase II randomised clinical trial," Brit. Med. J. **350**, g7635 (2015).
3. A. Pellicer, G. Greisen, M. Benders, O. Claris, E. Dempsey, M. Fumagally, C. Gluud, C. Hagmann, L. HellstrÃűm-Westas, S. Hyttel-Sorensen, P. Lemmers, G. Naulaers, G. Pichler, C. Roll, F. van Bel, W. van Oeveren, M. Skoog, M. Wolf, and T. Austin, "The SafeBoosC phase II randomised clinical trial: a treatment guideline for targeted near-infrared-derived cerebral tissue oxygenation versus standard treatment in extremely preterm infants." Neonatology **104**, 171–178 (2013).
4. S. Hyttel-Sorensen, L. C. Sorensen, J. Riera, and G. Greisen, "Tissue oximetry: a comparison of mean values of regional tissue saturation, reproducibility and dynamic range of four NIRS-instruments on the human forearm," Biomed. Opt. Express **2**, 3047–3057 (2011).
5. N. Nagdyman, P. Ewert, B. Peters, O. Miera, T. Fleck, and F. Berger, "Comparison of different near-infrared spectroscopic cerebral oxygenation indices with central venous and jugular venous oxygenation saturation in children," Paediatr. Anaesth. **18**, 160–166 (2008).
6. R. N. Kreeger, C. Ramamoorthy, S. C. Nicolson, W. A. Ames, R. Hirsch, L. F. Peng, A. C. Glatz, K. D. Hill, J. Hoffman, J. Tomasson, and C. D. Kurth, "Evaluation of pediatric near-infrared cerebral oximeter for cardiac disease," Ann. Thorac. Surg. **94**, 1527–1533 (2012).
7. M. Wolf, G. Naulaers, F. van Bel, S. Kleiser, and G. Greisen, "A review of near infrared spectroscopy for term and preterm newborns," J. Near Infrared Spec. **20**, 43–55 (2012).
8. B. Meyer, C. Schaller, C. Frenkel, B. Ebeling, and J. Schramm, "Distributions of local oxygen saturation and its response to changes of mean arterial blood pressure in the cerebral cortex adjacent to arteriovenous malformations," Stroke **30**, 2623–2630 (1999).
9. H. D. Clay, "Validity and reliability of the sjo2 catheter in neurologically impaired patients: a critical review of the literature," J. Neurosci. Nurs. **32**, 194–203 (2000).
10. W. M. Coplin, G. E. O'Keefe, M. S. Grady, G. A. Grant, K. S. March, H. R. Winn, and A. M. Lam, "Thrombotic, infectious, and procedural complications of the jugular bulb catheter in the intensive care unit," Neurosurgery **41**, 101–107 (1997).

#262556 http://dx.doi.org/10.1364/BOE.7.002973
Journal © 2016 Received 8 Apr 2016; revised 31 May 2016; accepted 7 Jun 2016; published 11 Jul 2016

Biomedical Optics EXPRESS


11. A. Dullenkopf, B. Frey, O. Baenziger, A. Gerber, and M. Weiss, "Measurement of cerebral oxygenation state in anaesthetized children using the INVOS 5100 cerebral oximeter," Pediatr. Anesth. **13**, 384–391 (2003).
12. L. C. Sorensen and G. Greisen, "Precision of measurement of cerebral tissue oxygenation index using near-infrared spectroscopy in preterm neonates," J. Biomed. Opt. **11**, 054005 (2006).
13. C. Jenny, M. Biallas, I. Trajkovic, J.-C. FauchÃÍre, H. U. Bucher, and M. Wolf, "Reproducibility of cerebral tissue oxygen saturation measurements by near-infrared spectroscopy in newborn infants," J. Biomed. Opt. **16**, 097004 (2011).
14. M. Pocivalnik, G. Pichler, H. Zotter, N. Tax, W. Mueller, and B. Urlesberger, "Regional tissue oxygen saturation: comparability and reproducibility of different devices," J. Biomed. Opt. **16**, 057004 (2011).
15. L. M. Dix, F. van Bel, W. Baerts, and P. M. Lemmers, "Comparing near-infrared spectroscopy devices and their sensors for monitoring regional cerebral oxygen saturation in the neonate," Pediatr. Res. **74**, 557–563 (2013).
16. T. Szczapa, L. Karpinski, J. Moczko, M. Weindling, A. Kornacka, K. Wroblewska, A. Adamczak, A. Jopek, K. Chojnacka, and J. Gadzinowski, "Comparison of cerebral tissue oxygenation values in full term and preterm newborns by the simultaneous use of two near-infrared spectroscopy devices: an absolute and a relative trending oximeter," J. Biomed. Opt. **18**, 087006 (2013).
17. T. W. Hessel, S. Hyttel-Sorensen, and G. Greisen, "Cerebral oxygenation after birth - a comparison of INVOSÂő and FORE-SIGHTâĎć near-infrared spectroscopy oximeters," Acta Paediatr. **103**, 488–493 (2014).
18. A. Schneider, B. Minnich, E. Hofstaetter, C. Weisser, E. Hattinger-Jurgenssen, and M. Wald, "Comparison of four near-infrared spectroscopy devices shows that they are only suitable for monitoring cerebral oxygenation trends in preterm infants," Acta Paediatr. **103**, 934–938 (2014).
19. A. M. De Grand, S. J. Lomnes, D. S. Lee, M. Pietrzykowski, S. Ohnishi, T. G. Morgan, A. Gogbashian, R. G. Laurence, and J. V. Frangioni, "Tissue-like phantoms for near-infrared fluorescence imaging system assessment and the training of surgeons," J. Biomed. Opt. **11**, 014007 (2006).
20. S. Suzuki, S. Takasaki, T. Ozaki, and Y. Kobayashi, "Tissue oxygenation monitor using NIR spatially resolved spectroscopy," Proc. SPIE **3597**, 582–592 (1999).
21. C. D. Kurth, H. Liu, W. S. Thayer, and B. Chance, "A dynamic phantom brain model for near-infrared spectroscopy," Phys. Med. Biol. **40**, 2079–2092 (1995).
22. J. G. Kim and H. Liu, "Variation of haemoglobin extinction coefficients can cause errors in the determination of haemoglobin concentration measured by near-infrared spectroscopy," Phys. Med. Biol. **52**, 6295–6322 (2007).
23. E. L. Hull, M. G. Nichols, and T. H. Foster, "Quantitative broadband near-infrared spectroscopy of tissue-simulating phantoms containing erythrocytes," Phys. Med. Biol. **43**, 3381–3404 (1998).
24. A. Bozkurt, A. Rosen, H. Rosen, and B. Onaral, "A portable near infrared spectroscopy system for bedside monitoring of newborn brain," Biomed. Eng. Online **4**, 29 (2005).
25. J. Kraitl, U. Timm, and H. Ewald, "Non-invasive measurement of blood and tissue parameters based on vis-nir spectroscopy," Proc. SPIE **8591**, 859105 (2013).
26. S. Hyttel-Sorensen, S. Kleiser, M. Wolf, and G. Greisen, "Calibration of a prototype NIRS oximeter against two commercial devices on a blood-lipid phantom," Biomed. Opt. Express **4**, 1662–1672 (2013).
27. S. Kleiser, S. Hyttel-Sorensen, G. Greisen, and M. Wolf, "Comparison of near-infrared oximeters in a liquid optical phantom with varying intralipid and blood content," Adv. Exp. Med. Biol. **876**, 413–418 (2016).
28. N. Nasseri, S. Kleiser, S. Reidt, and M. Wolf, "Local measurement of flap oxygen saturation; an application of visible light spectroscopy," Adv. Exp. Med. Biol. **876**, 391–397 (2016).
29. C. Kurth and B. Uher, "Cerebral hemoglobin and optical pathlength influence near-infrared spectroscopy measurement of cerebral oxygen saturation." Anesth. Analg. **84**, 1297–1305 (1997).
30. S. Hyttel-Sorensen, T. Austin, F. van Bel, M. Benders, O. Claris, E. M. Dempsey, M. Fumagalli, C. Gluud, C. Hagmann, L. Hellstrom-Westas, P. Lemmers, G. Naulaers, W. van Oeveren, A. Pellicer, G. Pichler, C. Roll, L. S. Stoy, M. Wolf, and G. Greisen, "Clinical use of cerebral oximetry in extremely preterm infants is feasible," Dan. Med. J. **60**, A4533 (2013).
31. "The INVOS system improving patient outcomes through cerebral/somatic oximetry," Tech. Rep. 11-PM-0256 MN21010, Medtronic, Inc., Minneapolis, MN, USA (2011).
32. "Model 8004CA, Instructions for use - english," Tech. Rep. 9539-001-02, Nonin Medical, Inc., 13700 1st Avenue North Plymouth, MN, 55441–55443, USA (2014).
33. "Model 8004CB-NA, Instructions for use - english," Tech. Rep. 9223-001-02, Nonin Medical, Inc., 13700 1st Avenue North Plymouth, MN, 55441–55443, USA (2014).
34. D. Hueber, S. Fantini, A. Cerussi, and B. Beniamino, "New optical probe designs for absolute (self-calibrating) NIR tissue hemoglobin measurements," Proc. SPIE **3597**, 618–631 (1999).
35. "Oxiplexts near infrared, non-invasive, tissue spectrometer," Tech. rep., ISS, Inc., 1602 Newton Drive Champaign, Illinois 61822, USA (2001).
36. R. Dash and J. Bassingthwaighte, "Erratum to: Blood $HbO_2$ and $HbCO_2$ dissociation curves at varied $O_2$, $CO_2$, $pH$, $2,3-DPG$ and $temperature$ levels," Ann. Biomed. Eng. **38**, 1683–1701 (2010).
37. R. Dash, B. Korman, and J. Bassingthwaighte, "Simple accurate mathematical models of blood $HbO_2$ and $HbCO_2$ dissociation curves at varied physiological conditions - Evaluation and comparison with other models," Eur. J. Appl. Physiol. **116**, 97–113 (2016).
38. T. Yoshida and S. S. Shevkoplyas, "Anaerobic storage of red blood cells," Blood Transfus. **8**, 220 – 236 (2010).

Biomedical Optics EXPRESS


39. A. J. Bellingham, J. C. Detter, and C. Lenfant, "Regulatory mechanisms of hemoglobin oxygen affinity in acidosis and alkalosis," J. Clin. Invest. **50**, 700–706 (1971).
40. W. G. Zijlstra, A. Buursma, and O. W. van Assendelft, *Visible and Near Infrared Absorption Spectra of Human and Animal Haemoglobin Determination and Application* (VSP: Utrecht, 2000).
41. R. Wodick and D. W. Luebbers, "Quantitative analysis of reflection spectra and other spectra of inhomogeneous light paths conducted in multi component systems with the aid of interval analysis part 1," Biol. Chem. **354**, 903–915 (1973).
42. J. Choi, M. Wolf, V. Toronov, U. Wolf, C. Polzonetti, D. Hueber, L. P. Safonova, R. Gupta, A. Michalos, W. Mantulin, and E. Gratton, "Noninvasive determination of the optical properties of adult brain: near-infrared spectroscopy approach," J. Biomed. Opt. **9**, 221–229 (2004).
43. A. Demel, K. Feilke, M. Wolf, C. F. Poets, and A. R. Franz, "Correlation between skin, bone, and cerebrospinal fluid layer thickness and optical coefficients measured by multidistance frequency-domain near-infrared spectroscopy in term and preterm infants," J. Biomed. Opt. **19**, 017004 (2014).
44. "SenSmart model X-100 universal oximetry system for pediatric patients," Tech. Rep. 10392-001-01, Nonin Medical, Inc., 13700 1st Avenue North Plymouth, MN, 55441-5443, USA (2014).
45. S. J. Arri, T. Muehlemann, M. Biallas, H. U. Bucher, and M. Wolf, "Precision of cerebral oxygenation and hemoglobin concentration measurements in neonates measured by near-infrared spectroscopy," J. Biomed. Opt. **16**, 047005 (2011).
46. S. Ijichi, T. Kusaka, K. Isobe, K. Okubo, K. Kawada, M. Namba, H. Okada, T. Nishida, T. Imai, and S. Itoh, "Developmental changes of optical properties in neonates determined by near-infrared time-resolved spectroscopy," Pediatr. Res. **58**, 568 – 573 (2005).
47. J. Dobbing and J. Sands, "Quantitative growth and development of human brain," Arch. Dis. Child. **48**, 757–767 (1973).
48. S. J. Matcher, P. J. Kirkpatrick, K. Nahid, M. Cope, and D. T. Delpy, "Absolute quantification methods in tissue near-infrared spectroscopy," Proc. SPIE **2389**, 486–495 (1995).
49. Y. Sakata, M. W. Abajian, M. O. Ripple, and R. Springett, "Measurement of the oxidation state of mitochondrial cytochrome c from the neocortex of the mammalian brain," Biomed. Opt. Express **3**, 1933–1946 (2012).
50. Y. Nosoh, "Absorption spectrum of actively respiring yeast cells," Arch. Biochem. Biophys. **105**, 439–445 (1964).
51. A. Demel, M. Wolf, C. F. Poets, and A. R. Franz, "Effect of different assumptions for brain water content on absolute measures of cerebral oxygenation determined by frequency-domain near-infrared spectroscopy in preterm infants: an observational study," BMC Pediatr. **14**, 1–6 (2014).


## 1. Introduction

In neonatology, infants born preterm are vulnerable to hypoxic and ischemic insults which lead to long-term disabilities. Diagnostic methods to early detect these conditions and prevent lesions are urgently needed. Optical methods such as near-infrared spectroscopy (NIRS) may be able to fulfill this need by assessing cerebral oxygenation non-invasively [1]. NIRS and visible light spectroscopy (VLS) utilize light to non-invasively and continuously assess tissue oxygen saturation ($StO_2$). Although there are a number of commercial NIRS oximeters available and entering the clinics, the evidence for clinical benefit is weak. A recent randomized clinical trial (SafeBoosC) carried out across Europe in 8 tertiary neonatal intensive care units including 166 extremely preterm infants, aimed to determine if it is possible to stabilize the cerebral oxygenation [2]. Cerebral oximetry was combined with a dedicated treatment guideline [3], providing a clinical intervention algorithm to assist neonatologists in clinical decision making when $StO_2$ was outside the target range of $55\% - 85\%$. Cerebral oxygenation was acquired by INVOS 5100C with adult SomaSensor or NIRO-200NX with small reusable probe, within 3 hours from birth. These two oximeters had previously been tested for comparability in-vivo [4]. The primary outcome measure of hypoxic and hyperoxic burden, was defined as the integral of the difference between $StO_2$ and the threshold over time outside the target range of $55\% - 85\%$ and and compared between the NIRS-visible group and a control group where NIRS was recorded but the data was not available to the clinician. In the trial the hypoxic/hyperoxic burden was reduced by more than 50%, paving the way for a future phase III study to show whether optical spectroscopy prevents brain lesions in preterm infants in the future [2]. However, despite substantial progress, several challenges need to be solved.

One problem is validation, i.e. do these oximeters measure $StO_2$ accurately? How can this be tested? $StO_2$ corresponds to the ratio of concentrations of oxy- and total hemoglobin

Biomedical Optics EXPRESS

($StO_2 = c_{O_2Hb}/c_{tHb}$, whereby $c_{tHb} = c_{O_2Hb} + c_{HHb}$). NIRS measures the average concentrations of oxyhemoglobin ($c_{O_2Hb}$) and deoxyhemoglobin ($c_{HHb}$) in the field of view of the light bundle and is sensitive to the hemoglobin in small blood vessels, i.e. arterioles, capillaries and venules.

A common approach is to validate $StO_2$ measured by the oximeter against co-oximetry of arterial and venous (e.g. jugular) blood samples [5, 6], similar to the validation procedure for pulse oximeters. Thereby often a proportional contribution of 30% arterial and 70% venous blood to the $StO_2$ is assumed. But this proportion cannot easily be measured and is likely to change over time and varies between tissues and subjects. [7] Moreover, venous samples truly representative of the optically measured tissue are difficult and risky to obtain. Jugular bulb represents global cerebral venous blood while the NIRS sensor samples only a small volume and it is known that brain oxygenation varies with location [8]. Furthermore, jugular blood is possibly contaminated by extracerebral drainage [9] and 40% of the patients suffer from thrombosis after jugular bulb catherterization [10]. Especially in preterm infants this procedure is not feasible for ethical reasons, which is probably true for adults as well. Therefore, it is impossible to establish the accuracy of the methods in-vivo from blood sample co-oximetry. At best these tests add plausibility [7].

Since there is no simple test so far and the specific $StO_2$ value depends on several assumptions, it is not surprising that oximeters from different manufacturers provide different $StO_2$ values as established by numerous studies [7, 11–18]. With the lack of a standard, the need arose to translate between different oximeters within and between trials (e.g. intervention thresholds in SafeBoosC). In-vivo vascular occlusions have previously been applied for this, because the induced ischemia allows characterization of the oximeter in a wide range of $StO_2$ [4]. This approach, however, is negatively affected by tissue in-homogeneity and physiological alteration over time.

To overcome this problem, oximeters can be characterized in-vitro in phantoms. This has the advantage of controllable optical properties with minimal variation, and can be constructed for the specific research question. Dye-based phantoms are mainly used for testing absorption measurements of oximeters, but are not suitable to assess oxygenation readings, as real hemoglobin is needed for this. Readings can be evaluated at multiple increments of $StO_2$ [19] or preferably in dynamic phantoms covering a continuous range of $StO_2$ [20–25]. Suzuki et al used a liquid phantom when introducing the NIRO-300 comparing NIRS measurements with co-oximetry as reference [20]. We have used a similar approach to directly compare oximeters as described previously [26–28]. Here we present an improved setup, where we minimized the vertical gradient in the oxygen content of the liquid phantom and improved the alignment of the oximeters which were simultaneously measuring oxygenation of the phantom. This ensures that the different oximeters measure the same oxygenation and absolute $StO_2$ values can truly be compared. In addition we added a second layer to the measurement setup, which simulated the neonatal skull. This setup, thus, is closer to the structure of a neonatal head.

Aims of the current paper are to derive mathematical equations to convert $StO_2$ measured by one oximeter to another one (INVOS adult/neonatal, Nonin neonatal, OxyPrem v1.3, OxiplexTS, and OxyVLS), to calculate oximeter-specific intervention thresholds for a phase III large scale follow-up trial of SafeBoosC, and to measure the inaccuracy of different oximeters due to variation of hemoglobin concentration ($c_{tHb}$) at these thresholds. The influence of hemoglobin is expected from phantom and piglet studies demonstrating a change in continous wave NIRS measurements as hemoglobin concentration changes [29].

## 2. Methods and materials

### 2.1. Oximeters

In the presented phantom experiment we included 4 NIRS oximeters with several sensors, one visible light oximeter and conducted oximetry based on the hemoglobin-oxygen dissociation

Biomedical Optics EXPRESS

curve, all measuring $StO_2$. We employed the following NIRS oximeters: OxiplexTS (ISS, Inc., Champaign, IL, USA), INVOS 5100C with Adult SomaSensor SAFB-SM and infant/neonatal OxyAlert NIRSensor CNN/SNN (Medtronic, Inc., Minneapolis, MN, USA), SenSmart Model X-100 Universal Oximetry System with adult 8004CA and non-adhesive neonatal/pediatric sensor 8004CB-NA (Nonin Medical, Inc., Plymouth, MN, USA) and OxyPrem v1.3 (in-house developed NIRS oximeter, University Hospital Zurich, Zurich, Switzerland).

As the intervention thresholds in SafeBoosC were determined from measurements on $>$ 400 preterm infants using INVOS 5100C with the adult SomaSensor [30], this adult sensor is included in this study. INVOS and Nonin neonatal sensors as well as Oxyprem v1.3 are expected to be used in phase III of SafeBoosC and hence need to be characterized. The Nonin adult sensor was added to see how it compares to its neonatal sensor. The OxiplexTS and OxyVLS (in-house developed VLS oximeter, University Hospital Zurich, Zurich, Switzerland) were included to compare the performance of frequency domain NIRS and oximetry based on visible light spectroscopy to the performance of continuous wave NIRS oximeters, respectively.

#### 2.1.1. NIRS oximeters

The **INVOS** system utilizes near-infrared light at 730 and 810$nm$, one source and two detectors at source-detector separations (SDS) of 30 and 40$mm$, providing two light paths. The INVOS 5100C provides "real-time data accuracy" which is claimed to be what others call "absolute" for certain clinical indications in patients $> 2.5kg$ [31] . The oximeter is approved for clinical use. **SenSmart** applies four wavelengths (730, 760, 810 and 870$nm$) and provides sensors for adults (SDS: 20 and 40$mm$) and neonates (SDS: 12.5 and 25$mm$). Both neonatal and adult sensors have two detector and two source locations, giving a total of four light paths providing absolute oxygen saturation for patients $< 40kg$ (neonatal/pediatric sensor) [32] and $> 40kg$ (adult sensor) [33]. The oximeter is approved for clinical use.

In **OxyPrem v1.3** we incorporated four wavelengths (690, 760, 805 and 830$nm$). It employs a self-calibrating principle [34] with 8 different light paths derived from two detectors and 4 different SDS (15, 20, 30 and 35$mm$). By applying this principle, the measured light intensity is independent of the sensitivity of the photo-detectors, light intensity at the source, light coupling factors and the influence of superficial tissue is reduced. The oximeter is not CE-marked but it has passed approval by medical device agencies on several occasions to acquire absolute $StO_2$ in humans for clinical trials.

**OxiplexTS** is a frequency domain NIRS oximeter with two wavelengths of 692 and 834$nm$ and a probe with SDS of 25, 30, 35 and 40$mm$ and 4 light paths. The oximeter modulates light at an RF frequency of $110MHz$ which enables measuring absolute absorption coefficient ($\mu_a$) and reduced scattering coefficient ($\mu_s'$) values. Subtraction of background absorbers and water content can be adjusted freely to account for different properties of tissues before calculation of $c_{O_2Hb}$ and $c_{HHb}$. The oximeter is CE-marked for research purposes and acquires absolute $StO_2$ [35].

#### 2.1.2. Oximetry based on the hemoglobin-oxygen dissociation curve ($StO_2$ derived from $pO_2$)

We calculated $StO_2$ derived from $pO_2$ based on a mathematical model assuming equilibrium binding of $O_2$ with hemoglobin inside red blood cells. This model has the form of a Hill type equation and enables invertible calculation of $StO_2$ based on partial pressure of oxygen ($pO_2$), partial pressure of carbon dioxide ($pCO_2$), $pH$, $temperature$, and 2,3-diphosphoglycerate ($2,3$-$DPG$) concentration [36, 37]. To produce accurate results $pO_2$, $pCO_2$, $pH$, and $temperature$ were measured and kept in a physiological range. We assumed $2,3$-$DPG \approx 0$ as is typical for stored blood [38]. The duration of each experiment was $< 4hr$, which excludes alterations in the amount of $2,3$-$DPG$ occuring after $4hr$ due to changes in $pH$ [39]. Since small changes in $pH$ and $temperature$ create large shifts in the oxygen hemoglobin dissociation curve, we kept $pH$

Biomedical Optics EXPRESS

close to the physiologically normal ($pH_{phys} = 7.4$) value by adding sodium bicarbonate buffer (SBB) and stabilized the temperature between $37-38°C$ by placing the phantom on a heating plate. We altered $pO_2$ between 0 and $\geq 10kPa$ to cover the full range of $StO_2$ ($0-100\%$). Table 1 indicates the sensors employed to derive $StO_2$ from $pO_2$ (manufactured by PreSens - Precision Sensing GmbH, Regensburg, Germany and Metrohm AG, Herisau, Switzerland).

Table 1. Sensors to measure partial pressure of oxygen ($pO_2$), partial pressure of carbon dioxide ($pCO_2$), $pH$, and $temperature$.

| | $\boldsymbol{pO_2}$ | $\boldsymbol{pCO_2}$ | $\boldsymbol{pH}$ | $\boldsymbol{temperature}$ |
|---|---|---|---|---|
| **transmitter** | Microx TX3 | $pCO_2$ mini v2 | - | Microx TX3 |
| **sensor** | NTH-PSt1 | flow through cell | 691 pH meter | pt1000 |
| **company** | Presens | Presens | Metrohm | Presens |

### 2.1.3. Oximetry based on visible light spectroscopy (OxyVLS)

We employed a Maya2000 Pro (Ocean Optics, Inc., Dunedin, FL, USA) spectrometer ($\approx 500-930nm$ spectral range, resolution $\approx 0.2nm$) combined with a tungsten halogen source ($360-2400nm$, $7W$, Ocean Optics) and a $400\mu m$ reflection probe (Ocean Optics), with approximately $2mm$ distance between light emission and detection. Spectra were acquired every $12s$. Based on VLS it is possible to determine the $StO_2$ [28]. Here we applied an improved method to measure $StO_2$. The wavelength range, from $520nm$ to $600nm$, is remarkable by oxyhemoglobin ($O_2Hb$) having two peaks ($\lambda = 542nm$ and $\lambda = 577nm$, data from [40]) and deoxyhemoglobin ($HHb$) having only one peak ($\lambda = 556nm$, data from [40]) [28]. Calculating $StO_2$ based on the distance between the peaks as described in [28] is prone to errors. In normal physiological conditions ($70\% < StO_2 < 85\%$) $1nm$ error in measurement of the distance between the peaks creates an error of $\approx 5-10\%$ in $StO_2$, which is too unstable. Moreover, when $StO2 < 30\%$ no peak is detectable, which previously prevented measurement of $StO_2 < 30\%$ [28]. Here we apply the "Interval analysis" technique to the spectrum of the liquid phantom in the range from 520 to $600nm$ to calculate $StO_2$. The details of this technique are depicted elsewhere [41]. As depicted in Fig. 1 we calculated the interval between two data points with the same optical density in the range from $\lambda = 520nm$ to $\lambda = 600nm$. By comparing it to the interval analysis signal of hemoglobin with known $StO_2$ (resolution: $0.1\%$ $StO_2$, data from [40]), we calculated the $StO_2$ of the liquid phantom. This method led to more stable results and enabled measurement of $StO_2 < 30\%$. Figure 2 shows the interval signal calculated for $O_2Hb$, i.e. $StO_2 = 100\%$.

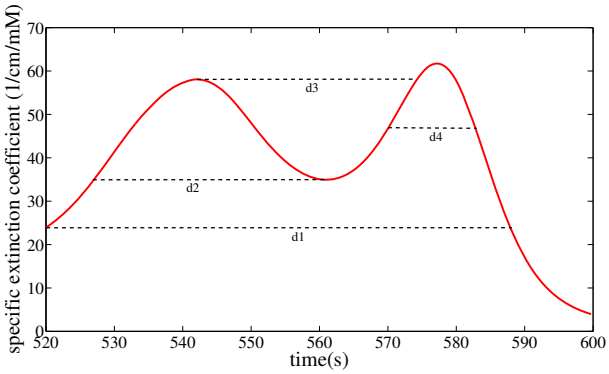


Fig. 1. Spectrum of $O_2Hb$. d1, d2, d3, and d4 depict the intervals for wavelengths of 520, 527, 542, and 570nm, respectively.

Biomedical Optics EXPRESS

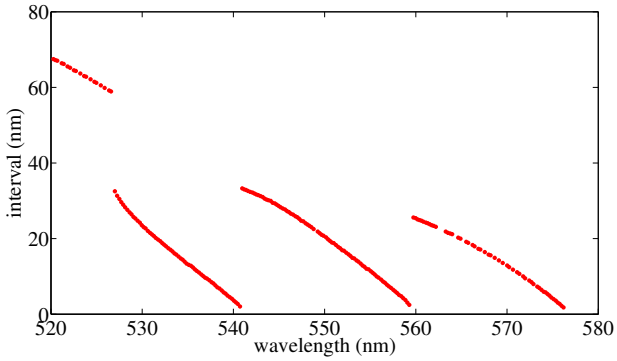


Fig. 2. Interval signal of $O_2Hb$.

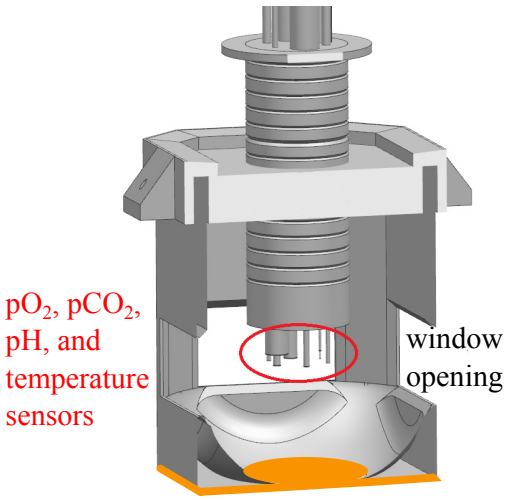


Fig. 3. (Phantom container (cut vertically in front). $pO_2$, $pCO_2$, $pH$, and *temperature* sensors were placed in the middle shaft. Sensors of NIRS oximeters were placed in the middle of the windows. The sensor of OxyVLS was immersed through a hole in the cap down to the middle of the windows. The cap effectively prevented oxygen and light entering into the phantom. The bottom plate of the phantom container was made of copper indicated in orange. For dimensions see Fig. 4.

## 2.2. *Measurement set-up and liquid phantom*

We prepared two liquid phantoms in a phantom container. The set-up is described below.

### 2.2.1. Phantom container

The phantom container was built in-house. We deployed the CAD tool NX (Siemens PLM Software) to design the phantom container and fabricated it from ABS plastic with a 3D-printer. The inside of the container was covered with bio-compatible epoxy to avoid cytotoxic effects. The phantom container was an irregular octagonal shape with four wide and four narrow side faces as is shown in Fig. 3 and 4. In these figures, the windows are not actually displayed, just the openings for them in the rigid container structure. This geometry enabled placing 4 NIRS oximeters on each wide side of the container. The phantom container had the following features:

Biomedical Optics EXPRESS

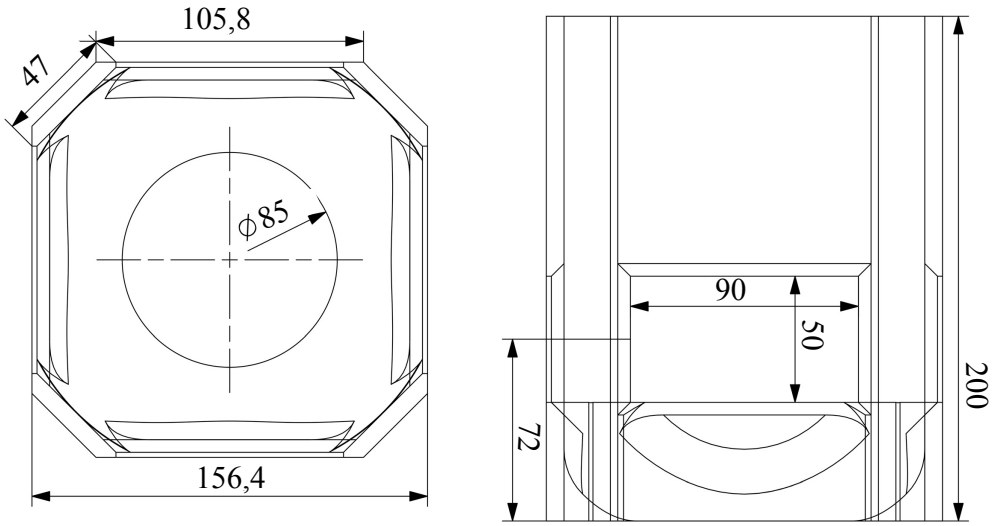


Fig. 4. Cross sections of the phantom container (windows not displayed) with outer dimensions of the container, window size and window separation in mm.

**Semi-infinite boundaries** The side faces of the container and holders pressing the sensors of the oximeters against the windows were built of absorbing material, thus effectively implementing a semi-infinite boundary condition. It also shielded the phantom from ambient light.

**No ambient oxygen diffusion** The cap of the container completely isolated the phantom from the ambient air. All the openings of the cap for placement of $pO_2$, $pCO_2$, $pH$, and *temperature* sensors as well as OxyVLS were sealed with silicone gaskets. Prior to measurement, we scanned the height of the phantom with a $pO_2$ sensor.

**High homogeneity and controlled temperature** We applied a magnetic stirrer, whose speed was set to $500rpm$ throughout the measurement, to effectively ensure homogeneity. If a gradient in the phantom exists, then it is due to $O_2$ diffusion from air through the phantom surface. With air on top of the liquid containing yeast, we measured a vertical gradient of less than $40Pa/cm$ which was negligible. Still we aligned all the sensors at the same height ($< \pm 0.5cm$) with their light path being horizontal to exclude the effect of any remaining vertical oxygen gradient. The bottom part of the phantom container constructed from copper enabled to place the phantom container on the hot plate of the stirrer, heating the liquid and thus keeping the phantom temperature constant.

**Optical cross-talk** The phantom container enabled simultaneous measurement with 4 different NIRS oximeters. The minimum distance between the two closest optodes of two different sensors was $7.5cm$, i.e. at least $3.5cm$ larger than the largest inter-optode distance of any sensor. This effectively prevented cross-talk.

**Windows simulating optical properties of the neonatal head** We cast 4 windows that reflected the optical properties of skull [42] with values of $\mu_a = 0.10\ cm^{-1}$ and $\mu_s' = 9.6\ cm^{-1}$ at $692nm$ and $\mu_a = 0.11\ cm^{-1}$ and $\mu_s' = 8.3\ cm^{-1}$ at $834nm$, which we expect to be a close approximation to the actual optical properties of the neonatal head. The windows were made from Silpuran 2420 silicone and were colored with $1.15ml/L$ Elastosil pigment paste FL RAL 9010 (white) (both Wacker Chemie AG, Munich, Germany) and $2.26mg/L$ carbon black powder (Alfa Aesar, Thermo Fisher (Kandel) GmbH, Karlsruhe, Germany). These windows were placed

Biomedical Optics EXPRESS

on each wide face of the container and served as the interface between the NIRS oximeters and the liquid phantom. The thickness of the windows was 2.5$mm$ which approximately reflected the thickness of skull in neonates [43].

All NIRS oximeters employed in this study claim to have algorithms which reduce the influence of superficial layers. Nonin neonatal as the oximeter with shortest source-detector separation (SDS) in our experiment has a penetration depth of 12.5$mm$ [44] which is 5 times the thickness of the windows. Based on this, we expect the windows to have only marginal influence on $StO_2$ readings. We nevertheless tried to make them similar to reality. It is obvious that influence of more superficial layers can more effectively be reduced. We therefore neglected the well perfused skin containing hemoglobin. The remaining layers, skull and cerebrospinal fluid, which contain very little hemoglobin are well represented by our single silicone layer which resembles data obtained in-vivo only showing two layers: outer and inner (brain) [42].We thus expect the phantom to be a good approximation for the neonatal head. Although the skull is perfused, its hemoglobin content is much lower compared to the brain itself. As a result windows with no blood are still a good estimation of the reality. In the future, the measurement set-up could possibly be further improved: Developing windows which simulate the whole spectrum of hemoglobin by means of mixing blood with the windows seems possible [19] and might be even a closer approximation to the reality. But stability of blood cells during the production procedure of the windows and long term stability would first have to be verified.

#### 2.2.2. Oxygen supply

A tube from an industrial oxygen tank ($O_2 \geq 99.5\%$, PanGas AG, Dagmersellen, Switzerland) through a flow-meter was immersed to approximately 2$cm$ above the bottom of the container in order to provide oxygen to the phantom when needed.

#### 2.2.3. Liquid phantom

The liquid phantom consisted of phosphate-buffered saline (PBS, after Kreis, $pH = 7.4$, Kantonsapotheke Zurich, Zurich, Switzerland), human blood from expired human erythrocyte concentrate bags (expiry date $<$ 2 months, total hemoglobin concentration: $tHb = 220g/L$, hematocrite: $htc = 67\%$), Intralipid 20% solution (IL) (Fresenius Kabi AG, Bad Homburg, Germany), sodium bicarbonate buffer 8.4% (1 $mmol/ml$) (SBB) (B. Braun Medical AG, Sempach, Switzerland), and glucose 50% (AlleMan Pharma GmbH, Reutlingen, Germany). Fresh baker's yeast was added, when needed, to deoxygenate the hemoglobin. The optical properties of the liquid phantom resembled that of the neonatal brain [45, 46]. We aimed at $\mu_s'$ of 5.5 ($cm^{-1}$) and obtained an average $\mu_s'$ of 6.8 $cm^{-1}$ (692$nm$) and 5.4 $cm^{-1}$ (834$nm$) (measured by OxiplexTS). Since $c_{tHb}$ is highly variable between neonates, we introduced three mixtures with different levels of $c_{tHb}$ for each phantom: 25, 45, and 70$\mu M$. Table 2 indicates the ingredients of the liquid phantom. The phantom contained $\approx 98\%$ water which is only slightly more than up to 95% reported for neonatal brain tissue [47]. The IL content and hence the scattering was not changed. Theoretically this cancels out when calculating $StO_2$ out of $c_{O_2Hb}$ and $c_{tHb}$ with only the wavelength dependency remaining [48]. A previous phantom study confirmed this [27].

For liquid phantoms containing hemoglobin there are two possibilities to reversibly deoxygenate the hemoglobin. The first way is via gas-exchange, either by $N_2$ in-flow or by a membrane oxygenator [26]. The second way is by adding small quantities of respiring yeast into the phantom [20, 27, 28]. Deoxygenating by $N_2$ in-flow is relatively slow for large phantom volumes and also creates in-homogeneity which may invalidate the results when lowering $StO_2$. This method, however, works if the $StO_2$ of the phantom is fixed at a certain level but this fixation requires a sophisticated set-up which prevents any $O_2$ diffusion from the ambient air into the phantom. The inhomogeneity problem is not solved by using a membrane oxygenator

Biomedical Optics EXPRESS

because at the inlet, blood with a different level of oxygenation than that of the bulk phantom enters and is a source of inhomogeneity. A simpler alternative for deoxygenating hemoglobin is to add yeast. Yeast in the phantom, if stirred well, causes distributed oxygen consumption and therefore prevents inhomogeneity. This method is also much faster and therefore we decided to deoxygenate the phantom by adding yeast. For oxygenating, however, we used $O_2$ in-flow which might have created inhomogeneity but this is not an issue as we only used the data while deoxygenating the phantom.

Table 2. Ingredients of the liquid phantom. Yeast 1 indicates the amount of yeast in phantom 1 and yeast 2, the amount of yeast in phantom 2.

| **mixture** | **PBS** ($mL$) | **blood** ($mL$) | **IL** ($mL$) | **SBB** ($mL$) | **glucose** ($mL$) | **yeast 1** (g) | **yeast 2** (g) | $htc$ (%) | $c_{tHb}$ ($\mu M$) |
|---|---|---|---|---|---|---|---|---|---|
| $no.1$ | 2500 | 20 | 74 | 15 | 3 | 1.5 | 3 | 0.52 | $26.32 \approx 25$ |
| $no.2$ | 2500 | 33.5 | 74 | 25 | 6 | 1.5 | 3 | 0.86 | $43.85 \approx 45$ |
| $no.3$ | 2500 | 53.5 | 74 | 35 | 9 | 3 | 3 | 1.36 | $69.5 \approx 70$ |

### 2.3. Measurement protocol

We prepared two liquid phantoms with three mixtures each (table 2). Phantom 1 and phantom 2 had the same ingredients (except from the amount of yeast). $pO_2$, $pCO_2$, $pH$, and *temperature* sensors, OxyVLS, OxyPrem v1.3 and OxiplexTS were employed in both phantoms. Additionally, Nonin adult and INVOS adult oximeters were employed in phantom 1, whereas Nonin neonatal and INVOS neonatal were employed in phantom 2. We started deoxygenating the hemoglobin by adding yeast and re-oxygenated it by providing $O_2$ into the phantom. The measurement started at $pH = 7.4$. During the measurement, $pH$ gradually decreased due to $CO_2$ accumulation in the phantom (produced by yeast). In order to keep the $pH$ close to $pH_{phys} = 7.4$, we gave initially $15ml$ and additionally two times $10mL$ SBB to each phantom. We added more glucose ($+3mL$) to both phantoms when adding more blood (leading to the next mixture). Table 3 summarizes the procedure for phantom 1, and phantom 2. To increase the speed of deoxygenation, we added more yeast ($+1.5g$) for mixture no. 3 in phantom 1.

Table 3. Procedure of changing the $StO_2$ level of phantom 1 and phantom 2.

| **step** | **phantom1** | **phantom2** |
|---|---|---|
| 1. | Prepare mixture no.1 as described in table 2 | |
| 2. | Start stirring (500 rpm) | |
| 3. | Start the measurement (initial oxygenation is high) | |
| 4. | Add 1.5$g$ yeast. | Add 3$g$ yeast. |
| 5. | Wait until $pO_2$ reaches the low plateau | |
| 6. | Provide $2L/min$ flow of $O_2$ and stop when $pO_2 > 10kPa$ | |
| 7. | Wait for low plateau of $pO_2$ | ——— |
| 8. | Add more blood and $3mL$ glucose | |
| 9. | Wait for low $pO_2$ plateau. | |
| 10. | Repeat 6-9 for mixture no.2. | Repeat 6-8 for mixture no. 2. |
| 11. | Add 1.5$g$ yeast | ——— |
| 12. | Repeat 6-7 for mixture no.3. | Repeat 9 for mixture no. 3. |

Biomedical Optics EXPRESS

We constantly monitored $pO_2$, $pCO_2$, $pH$, and $temperature$ during the course of the measurement. Table 4 shows the range of $pO_2$, $pCO_2$, $pH$, and $temperature$ during the measurement for phantom 1 and phantom 2.

Table 4. Range of $pCO_2$, $pH$, and $temperature$ in phantom 1 and in phantom 2.

| | $\boldsymbol{pCO_2}(kPa)$ | | | $\boldsymbol{pH}$ | | | $\boldsymbol{temperature}(^\circ C)$ | | |
|---|---|---|---|---|---|---|---|---|---|
| | min | mean | max | min | mean | max | min | mean | max |
| **phantom 1** | 1.88 | 4.31 | 9.23 | 7.09 | 7.28 | 7.52 | 37.50 | 37.81 | 38.00 |
| **phantom 2** | 0.68 | 7.48 | 14.9 | 7.06 | 7.29 | 7.54 | 35.80 | 36.91 | 38.40 |

### 2.4. Data processing

We applied a moving average filter over 3 samples on OxyVLS data. For all other oximeters, raw $StO_2$ values were recorded. For INVOS, Nonin, OxyPrem v1.3 and OxiplexTS oximeters we placed several event markers throughout the measurements which were used for alignment of the different time-series. We re-sampled the data from all devices to $\frac{1}{12}Hz$ (sampling rate) and created time-series for all devices on a common time base.We inspected the data visually thereafter to find the synchronization precision. This precision was higher than one sample. This means that the maximum time lag that could occur between samples in repeated measurements was $12s$. Obvious artifacts were removed, i.e data with saturated detector for the OxiplexTS. We applied $1^{st}$ degree polynomial fits (based on lowest least square error) to calculate the relation between $StO_2$ measured by different oximeters during deoxygenations in the range of $16\% \leq StO_2 \leq 94\%$.

## 3. Results

Figures 5 and 6 show the $StO_2$ time series of the oximeters in phantom 1 and phantom 2, respectively. We increased $c_{tHb}$ step-wise: $c_{tHb} = 25\mu M$, $45\mu M$ and $70\mu M$ (table 2) as depicted in Fig. 5 and 6 by the intensity of background red color. The changes in oxygenation are visible.

Figures 7-11 show in scatter plots how each individual oximeter compared to OxiplexTS at $c_{tHb} = 25\mu M$, $45\mu M$ and $70\mu M$. OxiplexTS was chosen as reference because the $StO_2$ derived from $pO_2$ shows a drift in phantom 2 (Fig. 6) and because it is commercially available (in contrast to OxyVLS). The choice of reference is discussed in detail in section 4.1. Equations of the linear fits and coefficients of determination ($R^2$) are given in the figure captions ($StO_{2,device} = a * StO_{2,OxiplexTS} + b$). Only data-points while deoxygenating (no oxygen flow) within the gray rectangle ($16 \leq StO_2 \leq 94\%$) were included for fitting. A dark gray polygon is defined by the fitting lines for $25\mu M$ and $70\mu M$. The area of this polygon is different for all oximeters and qualitatively reflects dependence of the $StO_2$ reading on $c_{tHb}$. For OxyPrem v1.3 and OxyVLS there are more data-points, because these sensors were present in both phantoms. For oximeters from which data of more than one de-oxygenation was available, all available data was used to generate the fitting lines.

We do not report the results obtained from Nonin adult sensor, because we suspect that the sensor was not properly attached to the window of the phantom and data was implausible.

### 3.1. $StO_2$ conversion table and SafeBoosC intervention threshold

In table 5 we show coefficients for conversion of values recorded by one oximeter to the other (at $c_{tHb} = 45\mu M$). For the SafeBoosC and other trials, intervention thresholds were applied to study different interventions. Here it is important to take into consideration the difference in values that oximeters display for a specific $StO_2$. E.g. in the SafeBoosC trial the hypoxic threshold was 55% and the hyperoxic 85%, based on values measured by the INVOS adult

Biomedical Optics EXPRESS

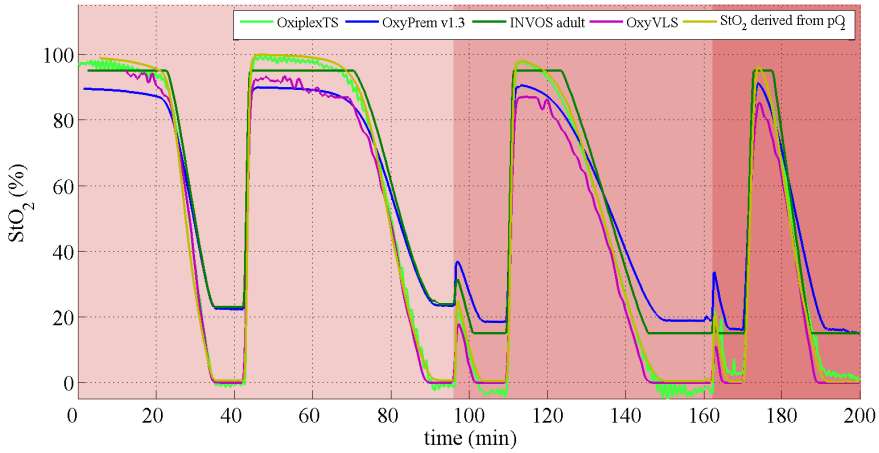


Fig. 5. Time series of the $StO_2$ readings of oximeters in phantom 1 with blood content expressed as the background red color.

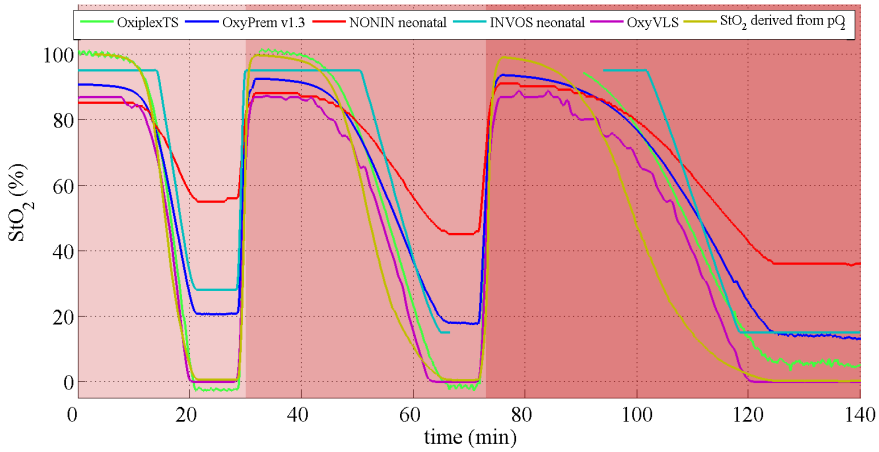


Fig. 6. Time series of the $StO_2$ readings of oximeters in phantom 2 with blood content expressed as the background red color.

Biomedical Optics EXPRESS

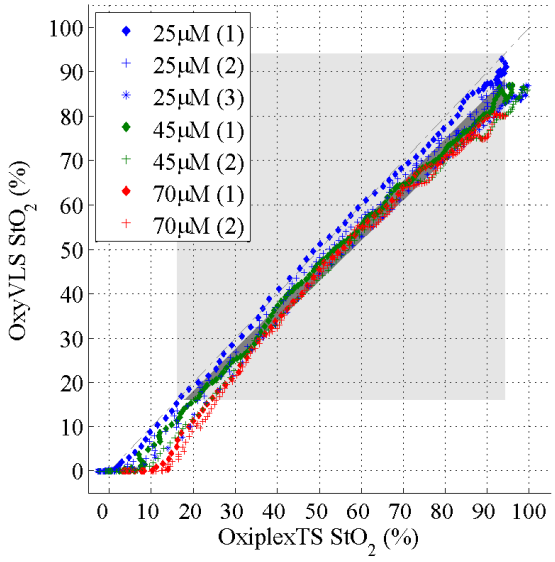


Fig. 7. OxyVLS versus OxiplexTS for $c_{tHb} = 25\mu M$ ($y = 0.947x - 0.9, R^2 = 0.9843$,), $45\mu M$ ($y = 0.913x - 1.5, R^2 = 0.9907$) and $70\mu M$ ($y = 0.912x - 2.7, R^2 = 0.9892$). $25\mu M(1)$, $25\mu M(2)$, $45\mu M(1)$ and $70\mu M(1)$ were measured on phantom 1, $25\mu M(3)$, $45\mu M(2)$ and $70\mu M(2)$ were measured on phantom 2.

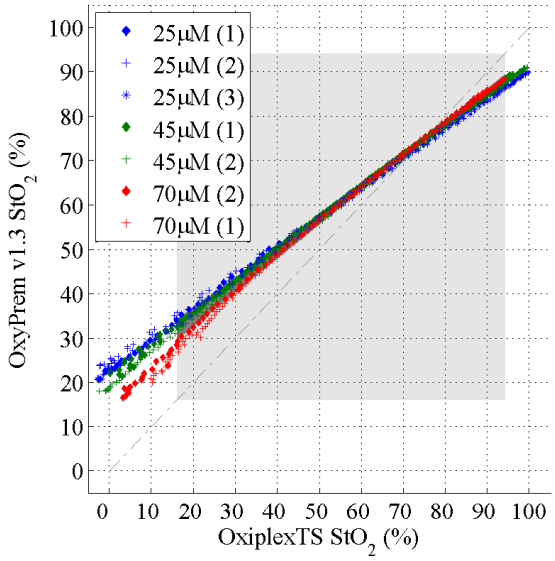


Fig. 8. OxyPrem v1.3 versus OxiplexTS for $c_{tHb} = 25\mu M$ ($y = 0.675x + 23.5, R^2 = 0.9985$), $45\mu M$ ($y = 0.709x + 21.3, R^2 = 0.9990$) and $70\mu M$ ($y = 0.768x + 17.2, R^2 = 0.9978$). $25\mu M(1)$, $25\mu M(2)$, $45\mu M(1)$ and $70\mu M(1)$ were measured on phantom 1, $25\mu M(3)$, $45\mu M(2)$ and $70\mu M(2)$ were measured on phantom 2.

Biomedical Optics EXPRESS

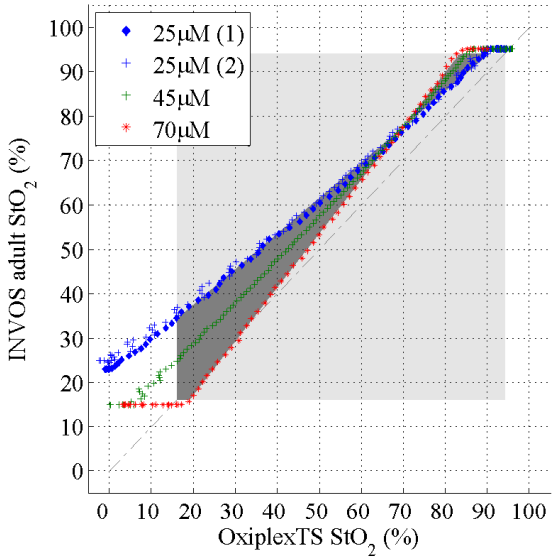


Fig. 9. INVOS adult versus OxiplexTS for $c_{tHb} = 25\mu M$ ($y = 0.802x + 21.5, R^2 = 0.9973$), $45\mu M$ ($y = 0.996x + 8.1, R^2 = 0.9994$) and $70\mu M$ ($y = 1.213x - 7.1, R^2 = 0.9997$). All data was measured on phantom 1.

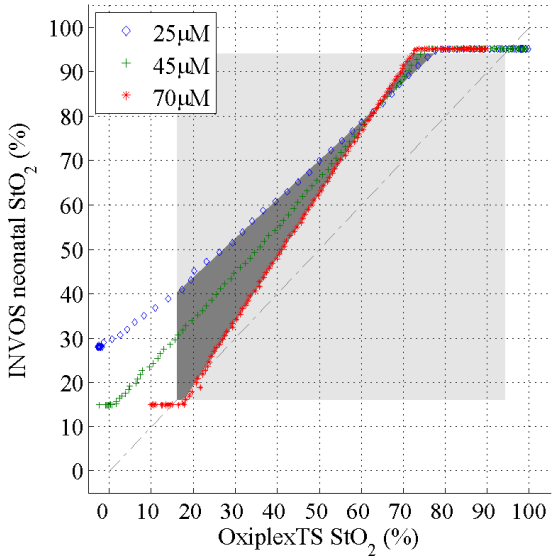


Fig. 10. INVOS neonatal versus OxiplexTS for $c_{tHb} = 25\mu M$ ($y = 0.877x + 26.2, R^2 = 0.9991$), $45\mu M$ ($y = 1.094x + 11.8, R^2 = 0.9994$) and $70\mu M$ ($y = 1.438x - 9.4, R^2 = 0.9995$). All data was measured on phantom 2.

Biomedical Optics EXPRESS

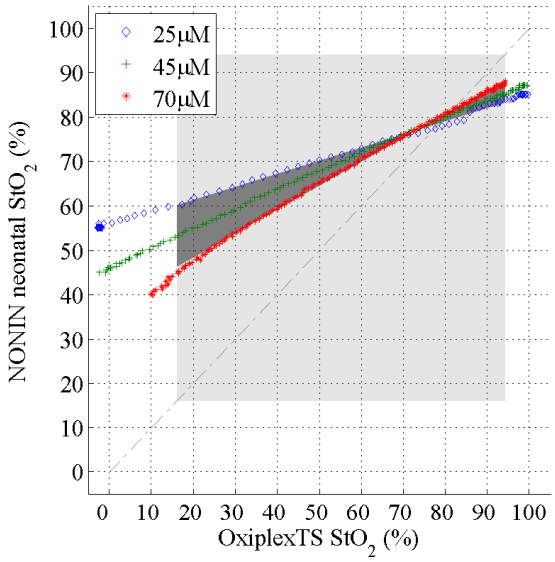


Fig. 11. Nonin neonatal versus OxiplexTS for $c_{tHb} = 25\mu M$ ($y = 0.295x + 55.4, R^2 = 0.9940$), $45\mu M$ ($y = 0.410x + 47.1, R^2 = 0.9989$) and $70\mu M$ ($y = 0.539x + 37.6, R^2 = 0.9982$). All data was measured on phantom 2.

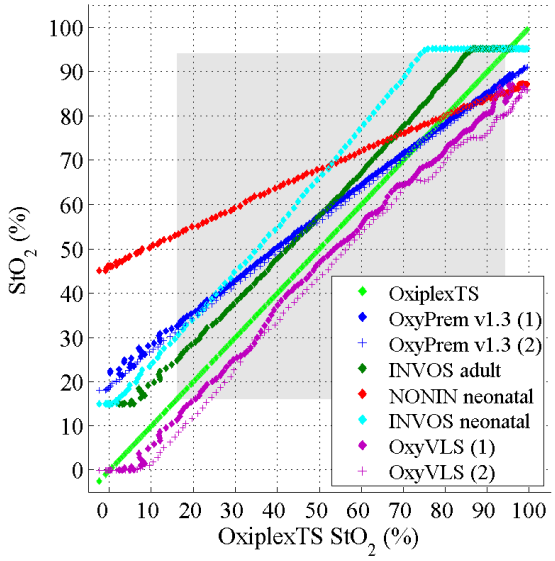


Fig. 12. All oximeters versus OxiplexTS for $c_{tHb} = 45\mu M$. The vertical black lines indicate INVOS adult measuring $StO_2 = 55\%$ and $85\%$. (1) and (2) indicate the phantom on which the data was acquired for OxyPrem v1.3 and OxyVLS.

Biomedical Optics EXPRESS

oximeter [2]. Table 6 presents what these thresholds correspond to for other NIRS oximeters. The table also contains the uncertainty range of $StO_2$ readings due to variations in $c_{tHb}$ at these thresholds. Figure 12 displays for $c_{tHb} = 45\mu M$ the $StO_2$ measured by all oximeters compared to the OxiplexTS.

Table 5. Coefficients for linear $StO_2(\%)$ conversion from any oximeter to the scale of any other oximeter: $StO_{2,to} = a * StO_{2,from} + b$.

| **to →** | **OxiplexTS** | | **OxyPrem v1.3** | | **INVOS adult** | | **INVOS neonatal** | | **Nonin neonatal** | | **OxyVLS** | |
|---|---|---|---|---|---|---|---|---|---|---|---|---|
| **from ↓** | *b* | *a* | *b* | *a* | *b* | *a* | *b* | *a* | *b* | *a* | *b* | *a* |
| **OxiplexTS** | 0.0 | 1.00 | 21.3 | 0.71 | 8.1 | 1.00 | 11.8 | 1.09 | 47.1 | 0.41 | -1.5 | 0.91 |
| **OxyPrem v1.3** | -30.0 | 1.41 | 0.0 | 1.00 | -21.9 | 1.41 | -21.0 | 1.54 | 34.8 | 0.58 | -28.9 | 1.29 |
| **INVOS adult** | -8.1 | 1.00 | 15.6 | 0.71 | 0.0 | 1.00 | 3.0 | 1.10 | 43.8 | 0.41 | -8.9 | 0.92 |
| **INVOS neonatal** | -10.8 | 0.91 | 13.6 | 0.65 | -2.7 | 0.91 | 0.0 | 1.00 | 42.7 | 0.38 | -11.3 | 0.84 |
| **Nonin neonatal** | -114.9 | 2.44 | -60.1 | 1.73 | -106.4 | 2.43 | -113.8 | 2.67 | 0.0 | 1.00 | -106.4 | 2.23 |
| **OxyVLS** | 1.6 | 1.09 | 22.4 | 0.78 | 9.7 | 1.09 | 13.6 | 1.20 | 47.8 | 0.45 | 0.0 | 1.00 |

Table 6. Intervention thresholds for $c_{tHb} = 45\mu M$ and range of uncertainty due to variation of $c_{tHb}$ in the range of $25\mu M$ to $70\mu M$.

| | **INVOS adult** | **OxyPrem v1.3** | **INVOS neonatal** | **Nonin neonatal** |
|---|---|---|---|---|
| **hypoxic threshold** | 55% | 55% | 63% | 66% |
| **uncertainty range due to $c_{tHb}$** | 9.2% | 1.9% | 9.2% | 6.4% |
| **hyperoxic threshold** | 85% | 76% | 96% | 79% |
| **uncertainty range due to $c_{tHb}$** | 3.2% | 0.9% | 7.7% | 1% |

## 4. Discussion

As depicted in Fig. 5 and 6, OxiplexTS, OxyPrem v1.3, Nonin neonatal, INVOS adult and neonatal, $StO_2$ derived from $pO_2$ and OxyVLS responded consistently and linearly correlated to the induced changes in $StO_2$. Rise and decline of $StO_2$ occurred simultaneously, but different oximeters showed different absolute values, dynamic ranges and sensitivities. In phantom 1 curves became narrower because we initially kept the phantom at high $StO_2$ for $20min$ before adding yeast for the first time. For the second upper plateau in mixture no. 1, we oxygenated the phantom to $\approx 20kPa$. The upper plateaus in mixture no. 2 and 3 were oxygenated to only $11kPa$. The deoxygenation at mixture no. 3 was faster than the previous ones because the additional yeast ($1.5g$) outweighed the increased oxygen capacity of the phantom by increased $c_{tHb}$. In phantom 2 the experiment started at $pO_2 = 18kPa$ and we reoxygenated the phantom to $15kPa$ for mixture no. 2 and 3. The curves become broader because of the increased oxygen capacity by higher $c_{tHb}$.

### 4.1. Reference $StO_2$

In several previous phantom experiments co-oximetry has been applied, on samples taken from the phantom, to compare the output of the oximeters to. This is a straightforward procedure for experimental set-ups where $c_{tHb}$ is similar to that of human blood [29] . Inspired by Suzuki et al. [20] we tried to use co-oximetry by an ABL800 blood gas analyzer (Radiometer Medical ApS, Brønshøj, Denmark) as reference in a previous study [26] . This failed due to too low

Biomedical Optics EXPRESS

$c_{tHb}$ and too much turbidity (caused by Intralipid) in the sample. Centrifugation of the phantom sample yielded acceptable $C_{tHb}$, but the saturation values were not trustworthy as contamination by ambient air oxygen was probable.

Instead, in this study we attempted to do oximetry utilizing the hemoglobin-oxygen dissociation curve. We tried to obtain a reference $StO_2$ from $pO_2$, $pCO_2$, $pH$, $temperature$ and $2,3$-$DPG$ but it was only partially successful. In phantom 1 (Fig. 5) high correlation (0.999%) to OxiplexTS was observed. But in phantom 2 (Fig. 6), there was a large deviation between this $StO_2$ derived from $pO_2$ and $StO_2$ from OxiplexTS, which increased over time. Later we identified the $pH$ sensor as the cause of the problem with drifts of up to $\Delta pH = \pm 0.2$ when immersed repeatedly into buffer solutions. As $pH$ plays a significant role, we believe that this created the observed drift between the $StO_2$ derived from $pO_2$ and OxiplexTS and OxyVLS values. Moreover, since a correct $StO_2$ measurement employing this approach is dependent on a precise measurement of $pO_2$, $pCO_2$, $pH$, $temperature$, and a correct assumption for $2,3$-$DPG$, we conclude that this approach is not practical for phantom measurements.

The second option to be set as the reference was OxyVLS. But OxyVLS is a built in-house oximeter which is still under development. It is also still not available in the market or for other research institutions. As a result, if it was chosen as the reference, reproducing the results by others would not have been possible.

OxiplexTS was adjusted to subtract the known background absorption of the phantom (98% water) before chromophore calculation and therefore did not show any dependence on $c_{tHb}$. It was in a good agreement with OxyVLS (correlation coefficient: 0.997), which inherently measures independent of $c_{tHb}$. In addition it was in good agreement with $StO_2$ derived from $pO_2$ in the first phantom, provides lower-noise $StO_2$ than OxyVLS at high sampling rate and more robust measurements than $StO_2$ derived from $pO_2$. Because of these reasons OxiplexTS was the best option and we set it as the reference for comparison of oximeters in this paper.

### 4.2. Plateaus, dynamic range, and sensitivity of the oximeters

The upper $StO_2$ plateau was different for all oximeters but it was unaffected by $c_{tHb}$. In Fig. 5 it seems that the upper plateau of $StO_2$ measured by OxyVLS decreased over time. One reason for this may be in the second upper plateau in mixture no. 1 we oxygenated the phantom to approx $20kPa$. The upper plateaus in mixture no. 2 and 3 were oxygenated to only $11kPa$. Additionally we added $1.5g$ more yeast to mixture no. 3. For these reasons we believe the phantom in mixture no. 2 and mixture no. 3 was not at its maximum oxygenation state before deoxygenation was started. Moreover, it may also be explained by the presence of cytochrome C in the medium, which was not included in the analysis and which changes the shape of the reflection spectrum of the turbid phantom, compared to the spectrum of pure hemoglobin in the range from $520nm$ to $600nm$ [49]. Yeast contains cytochrome C and was added in two steps [50]. In Fig. 6 this decrease was not observable, because the phantom was always oxygenated to $15kPa$ and the amount of yeast was also constant throughout the measurement. For all NIRS oximeters there were only marginal changes observable in the upper plateau.

The lower plateau of $StO_2$ (Fig. 5 and 6), in contrast, showed a dependence on $c_{tHb}$ level for all NIRS oximeters. The lower plateau of Oxyprem v1.3, INVOS adult, neonatal, and Nonin neonatal decreased as we increased $c_{tHb}$ from $25\mu M$ to $45\mu M$. The change was less pronounced when we increased $c_{tHb}$ from $45\mu M$ to $70\mu M$. Accordingly the dynamic range increased. The dynamic range of INVOS oximeters may appear less influenced by the $c_{tHb}$ change, but this is due to the oximeter not displaying values higher than 95% or lower than 15% $StO_2$ (clipping).

In Fig. 7-11 the lowest $R^2$ of the linear fits was $> 0.984$ which in our opinion is sufficient for comparison among oximeters. The maximum error due to linear regression in the fitting range is less than 4.5% with the highest values at the lower end of the $StO_2$ range which is not relevant for clinical decision-making. Within the range $55 < StO_2 < 85\%$ considered normal in

Biomedical Optics EXPRESS

SafeBoosC the data points are very well represented by linear regression.

In Fig. 7-11 the slope of each linear fit corresponds to the sensitivity of the oximeter to oxygenation changes with INVOS neonatal being the most and Nonin neonatal being the least sensitive at $c_{tHb} = 45\mu M$. There was a pronounced change in sensitivity for $c_{tHb} = 25\mu M$ compared to $70\mu M$ for Nonin neonatal (82%), INVOS adult (51%), and INVOS neonatal (64%), while OxyPrem v1.3 (14%) and OxyVLS (−4%) were much less dependent on $c_{tHb}$. Such an effect of $c_{tHb}$, although smaller (INVOS adult: 35%), was also observed in a previous study [27]. The reason for this difference is that in the present study, $c_{tHb}$ was much smaller ($phantom\ htc =$ 0.52% to 1.36% (corresponding to $c_{tHb} = 25\mu M$ and $70\mu M$) in the present study compared to $htc = 1\%$ to 2% in the previous study). Thus, in the previous study, the influence of background absorbers was smaller [27]. This explains the higher dependence of sensitivity of oximeters on the $c_{tHb}$ level in the current data.

This effect of $c_{tHb}$ on sensitivity, dynamic range, and lower plateaus depends on the technical specifications of the oximeters, such as how many and which wavelengths they incorporate, how other absorbers besides $O_2Hb$ and $HHb$ are being treated and if and how the wide spectra of LEDs compared to lasers have been handled. The number of wavelengths and the peak emission wavelengths of the oximeters are often reported by manufacturers, but the latter two points are not publicly available for most oximeters. Generally, the more wavelengths that are incorporated, the more precise the results will be. OxyPrem v1.3 incorporates 4 wavelengths which partially explains its decreased variability to changes in $c_{tHb}$ compared to INVOS sensors having 2 wavelengths only. However, variability of OxyPrem v1.3 is still less than that of the Nonin neonatal employing 4 wavelengths as well. The reason for that may be the contribution of the background absorbers which we reduced in OxyPrem v1.3. When $c_{tHb}$ and hence absorption caused by $c_{O_2Hb}$ and $c_{HHb}$ is low, e.g. in neonates, the relative contribution of such background absorbers is large and not negligible, as assumed by many oximeters. For the current phantom (table 2), lipids contributed ≈ 0.5% (being negligible) and water ≈ 98% of the volume. Except for a local absorption minimum of water at $810nm$, both, $O_2Hb$ and water generally show an increase of absorption in the range $680nm < \lambda < 920nm$. Lipid has low absorption in the wavelength range $600nm \leq \lambda \leq 870nm$. Above this wavelength, absorption increases rapidly. Therefore, depending on wavelengths employed, lipid might be relevant in human tissue with higher lipid contents and both, water and lipids, can possibly be mistaken as $O_2Hb$ by different oximeters. The result is an $c_{O_2Hb}$ offset even when $StO_2 = 0\%$. Since this error is wavelength dependent, the choice of wavelengths is crucial in reducing this effect. In OxyPrem v1.3 wavelengths of 690, 760, 805 and $830nm$ were selected based on simulations in which the wide emission spectrum of the LEDs were modeled by Gaussian distributions and with the aim to reduce the influence of water and lipid to a minimum. Figure 8 shows that we achieved this aim and OxyPrem v1.3 measures $StO_2$ with negligible variation over the wide range of neonatal brain $c_{tHb}$ levels because of the considerations mentioned above.

### 4.3. Reproducibility of the procedure

One of the aims of this paper was to provide mathematical equations to convert the results obtained by one oximeter to the results of the other oximeters (table 5). This will be valid only if the experiment is reproducible between the two phantoms. Oxyprem v1.3 and OxyVLS were present in both phantoms. In the first phantom we deoxygenated the phantom twice with the same amount of $c_{tHb}$. This led to two datasets with $c_{tHb} = 25\mu M$ in phantom 1. In addition we have a dataset in phantom 2. We applied individual linear fits to all three datasets in the range $16 \leq StO_2 \leq 94\%$. The standard deviations for slope (relative) and offset (absolute) coefficients were 0.89% and 0.86% for OxyPrem v1.3 while 2.28% and 2.17% for OxyVLS.

In dynamic measurements the correct alignment of the time-series influences the results of the comparison. We therefore aligned the data based on event markers and afterwards visually

Biomedical Optics EXPRESS

inspected the time-series. In the presented data, the highest rate of deoxygenation was $-8.3\%$ per minute at $c_{tHb} = 25\mu M$ in phantom 2. This means it takes $8min$ until hemoglobin reaches from $StO_2 = 94\%$ to $StO_2 = 16\%$. If we assume that alignment is off by one sample ($12s$), then this corresponds to a worst case error of $8.3\%/60s * 12s = 1.66\%$ which is well below the reproducibility of NIRS measurements in-vivo as reported in the literature [4, 7] and we consider this to be acceptable. We therefore conclude that the method was indeed reproducible.

### 4.4. Comparability of oximeters

The equations for conversion of $StO_2$ from one oximeter to the others assuming a typical neonate with $c_{tHb} = 45\mu M$ (table 5) enable researchers to quantitatively relate their own findings to data in the literature obtained by other oximeters. This means that clinicians do not have to wait until a specific observation has been made and reported with the same oximeter available to them. Especially for small patient groups such as preterm neonates this allows quicker implementation of new knowledge into practice.

### 4.5. SafeboosC intervention threshold

In table 6 we calculated oximeter-specific intervention thresholds for the clinical trial SafeBoosC corresponding to $StO_2 = 55\%$ and $85\%$ as measured by the INVOS adult oximeter for a typical neonate with $c_{tHb} = 45\mu M$. Our results show that the same oxygenation leads to quite different $StO_2$ values and intervention thresholds need to be adjusted to the specific sensor and oximeter accordingly. e.g. the hypoxic threshold has to be $11\%$ higher in case of the Nonin neonatal oximeter compared to the INVOS adult. OxyVLS has an $SDS \approx 2mm$ thus it is not suitable for brain monitoring. For this reason it is not included in table 6.

### 4.6. Implications of $c_{tHb}$ and background absorbers

A recent study reported that the variation of water content between infants leads to an uncertainty of $StO_2$ readings of up to $8\%$ [51], which is also supported by [27, 29]. This may systematically flaw clinical decisions. Variation of water content has the same effect on the relative contribution of background absorbers as of variation of $c_{tHb}$ as addressed above. The current experiment revealed a $c_{tHb}$ dependence at the SafeBoosC intervention thresholds (table 6). At the hypoxic threshold $StO_2$, INVOS adult and neonatal ($9.2\%$) showed the largest and OxyPrem v1.3 ($1.9\%$) the lowest dependence on $c_{tHb}$, i.e. uncertainty range of $StO_2$ readings.

In a trial with intervention thresholds, this means that oximeters with a high uncertainty effectively apply different $StO_2$ thresholds to patients with low $c_{tHb}$ level than for patients with high $c_{tHb}$ level. We expect that the reliability of such studies will be improved by oximeters providing more robust $StO_2$ readings, because they result in a more homogeneous threshold for the patient population.

## 5. Conclusion

In this paper we confirmed that different oximeters measured different $StO_2$ values on the same phantom simulating the neonatal head. We provided mathematical equations which translate data obtained from one oximeter to the others. Moreover, we have calculated the effect this has on intervention thresholds. We have additionally measured the dependence of $StO_2$ values on the $c_{tHb}$, which varies substantially between oximeters.

## Acknowledgments

The authors would like to thank Ranjan K. Dash (Medical College of Wisconsin, Department of Physiology) for valuable explanations to his $S_{HbO_2}$ model and for extending it to the case of several variables deviating from normal values at the same time [37]. The presented work was

Biomedical Optics EXPRESS

funded by The Danish Council for Strategic Research (grant number 00603-00482B) and the Nano-Tera projects ParaTex, ObeSense and NewbornCare and the Clinical Research Priority Program Tumor Oxygenation of the University of Zurich.